

# Neuron Dynamics of Two-compartment Traub Model for Hardware-based Emulation

Juan Carlos Moctezuma<sup>1,2</sup>, Jose Luis Nunez-Yanez<sup>2</sup> and Joseph P. McGeehan<sup>1</sup>

<sup>1</sup>CCR Group, Electronic Engineering, University of Bristol, Bristol, U.K.

<sup>2</sup>Micro Group, Electronic Engineering & Computer Science, University of Bristol, Bristol, U.K.

**Keywords:** Traub Model, Pinsky-rinzel Model, Bursting Analysis, Firing Analysis, Two-compartment Models, Neuron Modelling, Biophysically Accurate Hardware-model.

**Abstract:** The two-compartment Pinsky and Rinzel version of the Traub model offers a suitable solution for hardware-based emulation, since it has a good trade-off between biophysical accuracy and computational resources. Many applications based on conductance-based models require a proper characterization of the neuron behaviour in terms of its parameters, such as tuning firing parameters, changing parameters during learning processes, replication and analysis of neuron recordings, etc. This work presents a study of the dynamics of such model especially suitable for hardware-based development. The morphology of the neuron is taken into account while the analysis focuses primarily on the relation between the firing/bursting properties and the relevant parameters of the model, such as current applied and morphology of the cell. Two different applied currents were considered: short duration and long steady. Seven different types of burst patterns were detected and analysed. The transformation process of the membrane voltage when a long steady current varies was classified into five stages. Finally, examples of neuron recording replication using the present methodology are developed.

## 1 INTRODUCTION

Learning and memory process in any neuron or neural network is based on activity-dependant neuron responses. Modification of the physiological parameters is the tool to understand the functional and behavioural significance of this process; such parameters can modify patterns of neuronal firing/bursting and affect the behaviour in more high level functions (Dayan and Abbott 2001). For instance, several learning techniques and algorithms have been studied to achieve this goal and all of them are based on the modification of parameters in order to modify the neuron response (Grzywacz and Burgi 1998; Dayan and Abbott 2001).

Conductance-based modelling is not the exception, knowing the effects on the dynamics in the neuron is crucial to have control in the bursting and firing signals; which at the end, is the information that neurons will share through the system. Moreover, parameter's control in conductance-based model plays an important role in exploring the biological properties and dynamics mechanisms in real neurons or in the development of

control systems that lead to new feedback electrical stimulation for neural prostheses applications (Jiang et al. 2005; Fei et al. 2006).

The conductance-based models incorporate cellular detail at ion-channel level dynamics; this allows model biologically realistic neurons. One of the most important features of these models is that they are biophysical compatible and hence neuroscientists, biologists, psychologists can, at certain level, study the properties and co-relate directly parameters with their biological counterparts.

One of the most used conductance-based models, besides the well know Hodgkin-Huxley (H-H) (Hodgkin and Huxley 1952) is the Traub model (Traub et al. 1991) and its simplify two-compartment version P-R (Pinsky and Rinzel 1995), which take into account information about calcium ion channel  $Ca^{2+}$ . Calcium dynamic is another important element in the chemical and electrical behaviour in the neuron. This model can reproduce some burst patterns that H-H model cannot (Zhang et al. 2010). The two-compartment model includes two parts: a soma-like, which has the  $Na^+$  and  $K^+$

activated currents; and a distal dendrite-like, where  $\text{Ca}^{2+}$  activated and potassium  $\text{Ca}^{2+}$ -dependent currents are considered.

This research focus on the study of dynamic behaviour for the two-compartment P-R model with morphology information included. Most works related with this topic use theoretical and continuous model; however a hardware-based discrete model is not considered. Since our primary investigation is to develop biophysically compatible neuro-simulators and their hardware realization, it is important to keep good performance in order to have biological compatibility and reproduce consistent results from real nervous systems.

## 2 REVIEW OF PREVIOUS WORK

In this section, we review previous work done related to dynamic analysis in conductance-based models, particularly those using the Traub model. Studies of firing and bursting mechanisms in biological neurons have been widely studied during many years. Nerve cells can generate a variety of firing patterns *in vivo*, where repetitive burst, fast spikes, low frequency spikes, large calcium spikes, d-spikes, etc. have been recorded (Schwartzkroin 1975; Traub 1982).

In the original work of the P-R model (Pinsky and Rinzel 1995), an intrinsic bursting analysis when current is applied and excitatory synaptic interactions effect was performed. Another similar work is a piece-wise analysis where P-R model is separated in different stages and a dynamics study including burst initiation and somatic-dendrite ping pong is done (Coombes and Bressloff 2005). This work performs several reductions to the original model in order to make a phase-plane examination.

Bifurcation analysis is also a very useful approach to analyse dynamics in a neuron model as the parameters vary. Several works have studied this topic mainly for the well-known Hodgkin-Huxley model, in such works oscillations, stability in systems, bursting properties, spikes generation, temperature has been explored on this model (Rinzel and Miller 1980; Guckenheimer and Labouriau 1993; Wang et al. 2005; Fei et al. 2006). The bifurcation analysis becomes more difficult when the nonlinear systems have more than two parameters and equations to be considered at the same time.

The effect of the size in the soma in P-R model is studied and shows that the smaller the soma is, the faster and the more irregularly the neuron fires

(Feng and Li 2001). A modified version of the P-R model in order to have just two parameters variables in each compartment's equation is studied when capacitance changes and how complex bursting are generated (Kepecs and Wang 2000; Wang et al. 2012).

Several works using biological-compatible models have been developed in order to mimic real nervous systems behaviour; from study of single complex neurons to mimic complete biological systems (Khan and Miller 2010; Smaragdous et al. 2014). These researches highlight the importance of using this kind of models.

One important detail about previous work based on the P-R model is that the morphological properties are reduced to a simple parameter  $p$ , which indicates the proportion of the cell membrane area taken up by the soma. In the present work we extend this information by representing soma and dendrite as cylinder compartments where radius, length and axial resistivity are taken into account.

Traub model has been widely used in a variety of contexts, but little analysis has been performed for models of hardware-based applications and using the conductance-based approach.

## 3 THE P-R TRAUB MODEL FOR HARDWARE EMULATION

The P-R model is used in this work. This model offers a suitable trade-off between biophysical accuracy and computational feasibility to be developed in hardware (Zhang et al. 2010).

### 3.1 Specific Compartment Model

The cable equation and the multi-compartment theory describe the voltage change with respect to both variables: time and space. In the cable equation a segment of cell membrane is represented as a cylinder (cable); taking into consideration six currents: the capacitive  $i_c$ ; the total ionic-channels  $i_m$ ; the injected  $i_e$ ; and two more currents coming from adjacent segments  $i_{left}$  and  $i_{right}$  (Bower and Beeman 1998; Dayan and Abbott 2001). In this way, the cell membrane equation can be defined in terms of temporal and spatial variables  $t$  and  $x$ :

$$C_m \frac{\partial V}{\partial t} = I_e - I_m + \frac{1}{2a \cdot r_a} \cdot a^2 \frac{\partial^2 V}{\partial x^2} \quad (1)$$

Where  $r_a$  and  $C_m$  are the specific axial resistivity in unit of  $\text{K}\Omega\text{-cm}$  and the specific membrane

capacitance in unit of  $\mu\text{F}/\text{cm}^2$  respectively.  $I_e$  and  $I_m$  are the applied and ionic channel currents per unit area expressed in  $\mu\text{A}/\text{cm}^2$ . The cylindrical segment (compartment) having radius  $a$  and length  $dx=\Delta x$  (in units of cm) provides the morphological information.  $V$  is the membrane voltage in mV.

Because we need to represent this in a digital and computational way, the membrane voltage must be integrated numerically; to address this issue *multi-compartment* approach is used. Also, in order to reduce the PDE system to an ODE system, which is more suitable for numerical computation, the second order derivative in equation (1) is approximated by the discrete derivative version using the Taylor series expansion (Bower and Beeman 1998). Equation (2) shows a generic representation of the cell membrane for an arbitrary compartment  $j$ , where right compartment and left compartment are represented by  $j+1$  and  $j-1$  respectively.

$$C_m V'_j = I_e - I_m + \frac{a}{2r_a(\Delta x)^2} (V_{j-1} - 2V_j + V_{j+1}) \quad (2)$$

Note that  $V_j$  can represent either soma or dendrite compartment. Each one has its own ionic-channel current  $I_m$ , with  $\text{Na}^+$  and  $\text{K}^+$  ionic current components for soma and  $\text{Ca}^{2+}$ ,  $\text{K}^+$ \_AHP,  $\text{K}^+$ \_C current components for dendrite. Remind, every compartment has its own morphological dimensions. A complete description and specific variable values of the ionic-channel currents and the opening/closing rate functions  $\alpha$  and  $\beta$  can be found on (Pinsky and Rinzel 1995).

### 3.2 Numerical Method Solution

Because the model used for this work is intended to work in digital programming devices a numerical solution is needed. In (Zhang et al. 2010) it is shown that the best solution is the backward-Euler method, since it can maintain system stability regardless of the system structure and parameter selection. However this method brings high computational cost. The exponential-Euler method becomes unstable when the number of compartments increases or when a special combination of parameters is used, but it is more feasible in terms of hardware development. Since the model proposed has only two compartments and because just specific unusual combination of parameters cases makes the system unstable, exponential Euler method is the best option to implement.

Rewriting the cell equation (2) in a more convenient way:

$$C_m * V'_j = A - (B * V_j)$$

Where,

$$A = \psi_{GE} + I + \frac{a}{2r_a\Delta x^2} * (V_{j+1} + V_{j-1}) \quad (3)$$

$$B = \frac{a}{r_a\Delta x^2} + \psi_{Gtot}$$

Where  $\psi_{GE}, \psi_{Gtot}$  are the weighted averages of all ionic channels conductances. These two terms change according to the type of compartment (soma, dendrite or synapse); for instance, both terms for soma compartment are:  $\psi_{Gtot} = \overline{Gn\bar{a}} \cdot m_\infty^2 \cdot h + \overline{G_{k,DR}} \cdot p + \overline{G_{leak}}$  and  $\psi_{GE} = \overline{Gn\bar{a}} \cdot m_\infty^2 \cdot h \cdot E_{na} + \overline{G_{k,DR}} \cdot p \cdot E_k + \overline{G_{leak}} \cdot E_{leak}$ .

Applying exponential-Euler solution to equation (3), we can obtain the explicit solution for next time step given by equation (4):

$$V_{n+1} = \frac{A}{B} + \left( V_n - \frac{A}{B} \right) * e^{-B*dt/Cm} \quad (4)$$

### 3.3 Hardware Platform

A system on chip (SoC) platform has been developed where neuroprocessors form single or two-compartment neurons and control the connection between them. Such neuro-modules follow a scheme of state machines controllers (FSMCs), floating-point arithmetic units (FPALUs) and BRAMs to store internal results. Also, each neuroprocessor has associated a dual-port RAM (DRAM) in order to configure and control relevant parameters such as maximum conductance, input current, ions equilibrium potentials, geometric parameters, time step, configuration of state variables, etc. A neuroprocessor can be configured as a soma, dendrite or synapse compartment. For the purpose of this study a soma and dendrite neuroprocessor are used.

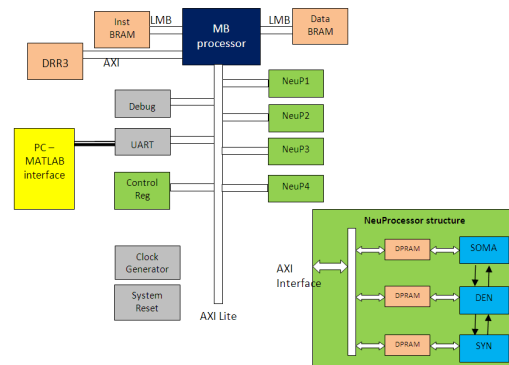


Figure 1: SoC system reconfigurable architecture.

The control and data paths are formed by a number of configurable FSMCs and FPALUs, respectively. The FSMCs are devised to fetch operands or forward computation results between the FPALUs and their associated RAMs. All temporary variables are saved in these internal memories that are located at the input ports of the FPALUs (Zhang et al. 2010; Moctezuma et al. 2013)

This platform is FPGA-based using an embedded microprocessor which is in charge of the control and communication task. In addition, there is a software firmware running which is able to manage the configuration of the neuroprocessors and make interconnections among them. This firmware is continuously receiving instructions from a MATLAB script running on a PC. Then commands can be send to configure the neuroprocessors, start a simulation and request results.

## 4 DYNAMICS ANALYSIS AND RESULTS

The dynamics analysis is divided into several stages, all of them related with the configuration of the neuron when current applied and geometric parameters change.

Following this scheme; the analysis is separated in four scenarios: burst classification; tuning the bursting neuron at resting state; short and long steady current applied and the impact of geometric dimensions. For all experiments, unless otherwise stated, the axial resistivity is 100 K $\Omega$ -cm, the diameters for soma and dendrite are 86.6  $\mu$ m and 5  $\mu$ m, respectively. The length of the cylindrical dendrite is set to 15  $\mu$ m, these values are consistent with measured experiments on hippocampal pyramidal cells (Traub 1982; Traub et al. 1994; Zhang et al. 2010).

### 4.1 Soma-Burst Classification

In order to understand and discern the neuron outputs in soma compartment, we have proposed seven different types of bursts for classification. Some of these bursts can be found also in biological experiments from neuron recordings (Traub 1982; Traub et al. 1991; Traub et al. 1994; Booth and Bose 2002). Figure 2 shows this classification.

Next, we defined each type of burst and explain their properties.

**SP:** Single Spike. **SP2:** Single main spike followed by other peaks. Normally they are sequences of two,

three, or four spikes. Dendrite main wide-spike is not well defined. **BA:** Classic Traub-burst, with initial sodium spike, followed by set of smooth oscillations during main dendrite wide-spike and ending with a final spike during the AHP current phase. Normally it has from two to four peaks. **BA2:** A Traub-burst shape with several pikes before the maximum of dendrite spike. Normally it has more than two spikes. The wide dendrite main spike starts to define. **BC:** Similar to SP2 but with a dendrite wide-spike defined. Normally it has 3 spikes. **BC2:** Collection of sequenced spikes but a little bump on a spike or small wide-pike is present. The main dendrite wide-spike is defined. **BD:** Classic Traub-burst shape, but with two principal set of spikes at the beginning and at the end enclosing the central part, which oscillates smoothly.

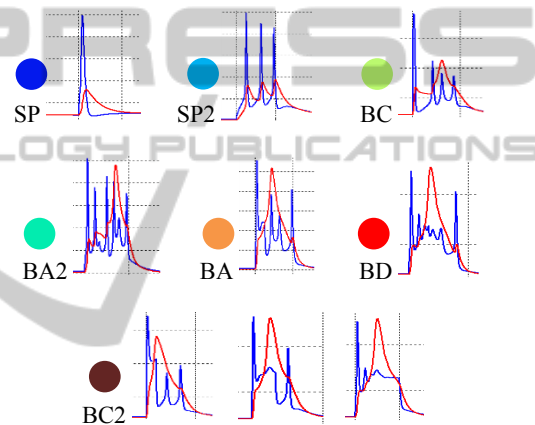


Figure 2: Burst classification with traces of soma (blue) and dendrite (red) compartments. Burst duration  $\approx$  20 msec.

### 4.2 Tuning Non-bursting at Resting State

The Traub-based model has a particular property that when no stimulus is applied to the cell membrane the neuron undergoes periodic bursting, albeit with very low frequency (Pinsky and Rinzel 1995) of around 0.6 Hz. However, this can be an undesirable behaviour when a learning process is involved; since normally, if a neuron is at its resting state, we do not expect the neuron to fire. To overcome this issue without affecting significantly the neuron dynamics, there are two options: to apply a large steady negative current or to slightly tune the leakage conductance. Table 1 shows the results obtained.

We found that a current of  $I_e = -0.85 \mu\text{A}/\text{cm}^2$  is enough to maintain the neuron at its resting state of -

70mV without firing. When current is bigger (more negative) than  $-1.7 \mu\text{A}/\text{cm}^2$  then resting potential tends to move away to less than  $-75\text{mV}$ .

The second option is reduce the leakage conductance. The original work of Pinsky-Rinsel and Traub, set a value of  $g_l=0.3$ ; table 1 shows that a slightly reduction of  $g_l$  at a value of  $0.285 \text{ mS}/\text{cm}^2$  is enough to eliminate the bursting and keep the resting potential close to  $-70 \text{ mV}$ . Moreover, if we decrease leakage conductance below  $0.28 \text{ mS}/\text{cm}^2$  the resting potential moves away to  $-75 \text{ mV}$ . In conclusion leakage conductance is highly sensitive to changes, but a value of  $0.285$  can overcome the initial bursting issue at the resting state without compromising the dynamic of the neuron.

Table 1: Current applied and leakage conductance tuning to eliminate initial bursting at resting stage.

Parameter	Value	Bursting	$V_{rest}$ (mV)
$I_e$ ( $\mu\text{A}/\text{cm}^2$ )	$> -0.85$	✓	$[-77 -70]$
	$-0.85$	-	$-71$
	$-1.00$	-	$-72$
	$< -1.70$	-	$< -75$
$g_l$ ( $\text{mS}/\text{cm}^2$ )	$0.3$	✓	$[-78 -70]$
	$> 0.3$	✓	
	$0.285$	-	$-72$
	$0.28$	-	$-74$
	$< 0.28$	-	$< -75$

### 4.3 Short and Long Steady Current Applied

In this section, we focus on finding the minimum stimulus needed to generate a single burst in the neuron, and how this short current modifies the quality of bursting in terms of outcome spikes. The second goal is to measure the outcomes from a long and steady current applied and determine the relation with the bursting behaviour of the neuron.

#### 4.3.1 Short Current Applied

The minimum short applied current needed to generate a single spike is  $8 \text{ nA}$  ( $136 \mu\text{A}/\text{cm}^2$ ) with a duration of  $0.5 \text{ msec}$ , see figure 3. With this duration, a current in the order of  $\text{mA}/\text{cm}^2$  per unit area in order to have a proper Traub bursting patron, however the spike amplitude overtakes  $150 \text{ mV}$ , which is not common amplitude for spikes. So the duration of  $0.5 \text{ msec}$  for the applied current is enough just to generate single spike but not Traub bursts such BA or BD type.

However if we increase the pulse duration, then the minimum applied current to generate a single

spike is shorter; for instance, with a  $20 \text{ msec}$  current pulse, it is necessary a  $0.6 \text{ nA}$  current to generate a SP spike. Hence if want a neuron to fire only single spikes then a pulse duration between  $0.5$  and  $3 \text{ msec}$  is ideal, see figure 3.

Following the same procedure, we run several experiments varying both current pulse duration and amplitude. Figure 3 shows the results obtained with the properties explained.

Another important characteristic about this model is that in order to have Traub-burst shapes like BA, BA2 or BD type, the current applied should last more than  $3 \text{ msec}$  and a range of  $[2 \text{ } 15] \text{ nA}$  should be used; and the larger the pulse is, the current applied becomes more “fine-grained” (narrow) as pulse duration increases, e.g. when pulse

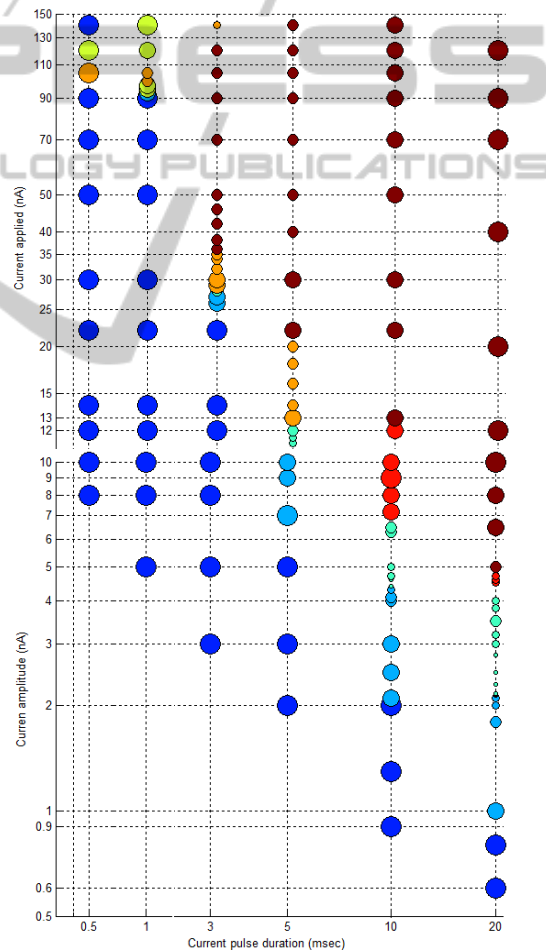


Figure 3: Soma membrane voltage response to different current pulse duration and amplitude. The colour in circles indicates the type of burst. The circle size indicates the number of spikes, where biggest blue circle is a single spike, followed by less big circles with 2 or 3 spikes; then medium size circles have a range of  $[4 \text{ } 6]$ ; and smallest circles have between 7 and 10 spikes.

duration is 20 msec, in order to have complex traub burst, a current between 4.4 and 4.7 nA is needed.

The duration of a Traub-burst when a current pulse is applied normally is about 20 msec. When a longer pulse is used then the burst duration takes the time that the pulse does. Also, we found that the current needs to be applied at least for 10 or 20 msec if we are interested in neuron fires between 5-10 times in the 20 msec window that the burst lasts.

Also we notice that there is an *evolution pattern* for this model. This evolution can be described by the following sequence: SP→SP2→BA2/BC→BA/BD→BC2. It starts with a single spike, then as the current increases, it generates two or three more spikes and the dendrite acts as passive. After that the dendrite starts to produce a main wide-spike caused by the ping-pong effect between the two compartments and a series of spikes are generated in the rising edge of the dendrite wide-spike. If we continue to increment the current, then the classic Traub-burst appears; but there is a point where this burst loses its shape due to a big current applied to component  $I_e$  dominates the equation and the neuron dynamic results in a first sodium spike followed by a smooth steady level of voltage.

These results can be applied to generate replicated behaviour for biological neurons recordings or to explore the neuron dynamics in a well-controlled environment. As an example consider two neuron output recordings from (Traub et al. 1991; Traub et al. 1994) works compared with the output from our model (figure 4). Using results from figure 3, the neuron behaviour can be controlled and analyse in a practical way.

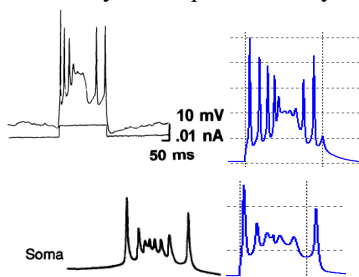


Figure 4: Burst replication of biological neuron recordings (left) with the two-compartment model proposed (right).

### 4.3.2 Long Steady Current Applied

Now we consider a long steady current applied during the whole simulation. When a constant current drives the neuron, spikes frequency appears rather than single burst patterns.

A set of experiments were developed varying current amplitude and principal stages of the process

as shown in figure 5. Meanwhile table 2 shows the relation of current vs frequency and stage transitions.

Table 2: Spike trains frequency and stages transition according to figure 4.

$I_e$ (nA)	Freq (Hz)	Spikes in Burst	Stage
0.0156	0.21	3	A
0.020	0.26	3	
0.035	0.34	3	
0.080	0.57	7	B
0.087	0.57	10	
0.087007	[50-41]	1	C
0.20	[33-58]	1	
0.60	[76-90]	1	
0.90	[100-111]	1	
1.20	[110-125]	1	
1.40	[112-130]	1	D
1.80	[112-140]	1	
2.50	[140-160]	1	
4.00	[200-250]	1	
4.50	80	1	E
5.00	0	0	

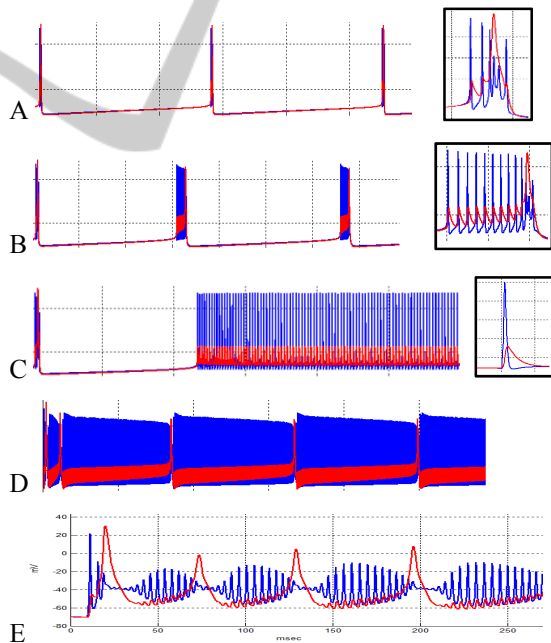


Figure 5: Different stages for a neuron soma (blue) and dendrite (red) response when steady current increase. Small left box indicates type of burst.

We distinguish five different stages according to the current increment. Stage A fires Traub-burst at very low frequency (VLF); in stage B the Traub-burst are preceded by several single spikes at VLF as well. There is a point at  $I_e=0.087007$  nA where this VLF burst disappears and a delayed spike train

appears (stage C), this spike train approaches the time of zero as current increases, at this stage we can have frequencies between 50 and 110 Hz (see table 2).

Then when the spike train reaches time zero, a low frequency envelope pattern is created, we can appreciate better this behaviour on dendrite output (red line) on figure 5-stage D; at this stage, frequencies of 250 Hz can be achieved. The amplitude of membrane voltage is reduced, decreasing the spikes frequency. In addition, the low frequency envelope pattern becomes more obvious (figure 5-stageE top). Finally the neuron output tends to become steady and the spike train disappears at  $I_e=5nA$  (figure 5-stageE bottom).

The minimum and maximum frequencies achieved with this model are 0.21 and 250 Hz respectively. And there is a cut current of 0.087 nA where traub-burst disappears and single spikes emerge.

#### 4.4 Effects of Geometric Properties

In this section we analyse the effects produced by changes in geometric properties of soma and dendrite. There are two main geometric parameters which affect the membrane voltage according to equation 3: the radius  $a$  and length  $\Delta x$ . Normally the soma has a sphere shape ( $a = \Delta x$ ) and dendrite has a cylinder form.

We took a well-defined Traub-burst type BD and analyze the changes appreciated when soma radius  $a$  and dendrite length  $\Delta x$  vary. Figure 6 shows the results and specifications for every trace.

There are four main effects when these two parameters vary:

- **Attenuation.** There is a general tendency of attenuation in the soma output as radius decreases; however on a dendrite output this effect is not so obvious for some cases. A major attenuation in the last part of neuron response is presented as dendrite length increases
- **Delay.** The bigger soma radius or dendrite length, the bigger delay for calcium concentration. In addition, we can observe how the number of pre-spikes or post-spikes are modified as this concentration moves during the 50 msec window. When both parameters are too big, there is a point when the dendrite output “disappears” (top-right figure 6), this effect is because the dendrite response is so delayed than the current pulse duration is not long enough to obtain such response.

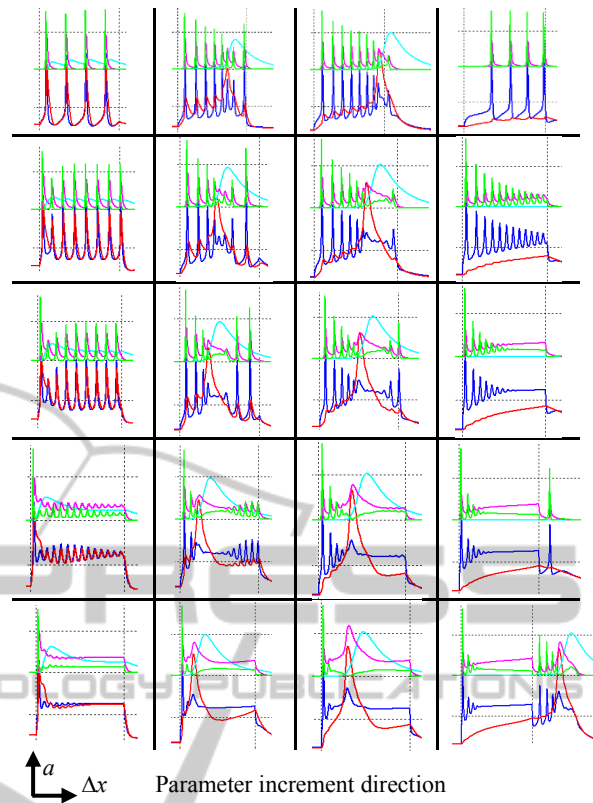


Figure 6: Different burst responses for a current pulse of 1.7 nA and 50 msec duration. Parameter values increase from bottom to top and from left to right directions. Range for radius soma  $a$  and dendrite length  $\Delta x$  are [15 60] and [5 50]  $\mu m$  respectively. Soma (blue) and dendrite (red) voltages in mV units. Calcium concentration (cyan), sodium current (green) and potassium-rectifier current (pink) in  $\mu A/cm^2$  are attenuated by factor of  $10^{-1}$ . The dendrite radius has a constant value of 3.6  $\mu m$ , since it is the parameter that changes the less. Every dashed square represents 50 units x 50 msec.

- **Spiking.** Normally the number of spikes increases more when the soma radius is bigger; also the dendrite wide-peak affects the number of pre-spikes and post-spikes change. This last consequence is related to the calcium concentration shifting. In addition, as the length of dendrite is smaller and the soma radius becomes bigger, then dendrite gets passive properties (top-left figure 6), active properties appear when the length increases.
- **Change in currents.** When soma radius is small then  $K^+$  rectifier current is bigger than  $Na^+$  one. However when the radius becomes bigger, then the current rules change. Because  $Na^+$  current is higher this causes the spiking effect to produces more spikes as well.

In order to analyse the morphological variation when a long steady current is applied, we set up two constant currents and vary soma radius and dendrite length. Again the dendrite radius compartment remains constant with a value of  $2.5 \mu\text{m}$ . The outcomes of the experiment are shown in figure 7.

For membrane voltage firing at VLF range, e.g. stage A or stage B (figure 7-a), the morphological parameters  $a$ -soma and  $\Delta x$ -dendrite have influence on the frequency and amplitude of the neuron output. Decrementing the dendrite length raises frequency; meanwhile decrementing the soma radius reduces the soma amplitude.

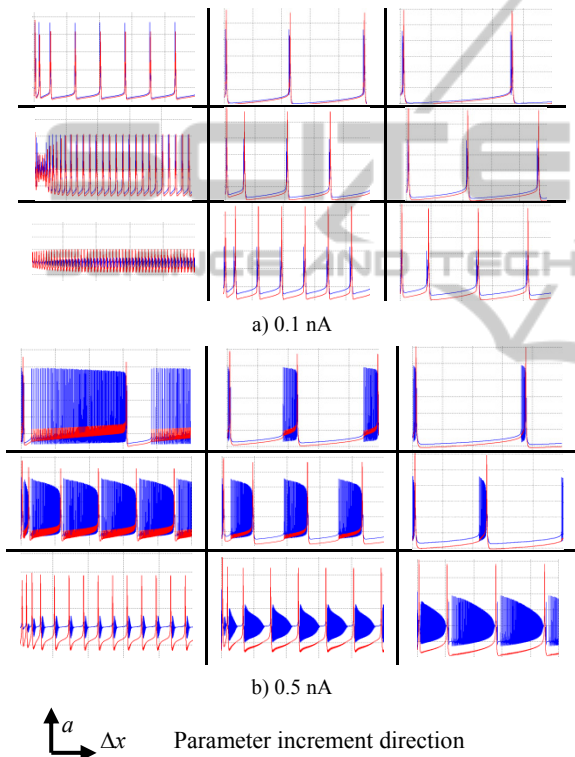


Figure 7: Soma (blue) and dendrite (red) traces responses for a long steady current of a)  $0.1\text{nA}$  and b)  $0.5\text{nA}$ . Parameter values increase from bottom to top and from left to right directions. Ranges for radius soma  $a$  are: a)  $[5\ 23]$  and b)  $[10\ 45] \mu\text{m}$ . Ranges for dendrite length  $\Delta x$  are: a)  $[10\ 30]$  and b)  $[10\ 50] \mu\text{m}$ . Every dashed square represents  $20\ \text{mV} \times 500\ \text{msec}$ .

When neuron fires in higher frequencies, e.g. stages C and D (figure 7-b), the effect is still the same, i.e. the bigger the radius the less the amplitude and the bigger the length, the less the frequency. In addition we can control the generation of periodic bursts, changing the number of spikes per burst according to morphological parameters tuning.

As an example consider the two recorded traces in figure 8 taken from a CA3 neuron (Traub et al. 1991) for two different currents. The two-compartment model was simulated with the same current values. The output of the proposed model is consistent with the recording value when the next morphological parameters are considered:  $a$ -soma =  $23.3 \mu\text{m}$ ,  $a$ -dendrite =  $2.5 \mu\text{m}$  and  $\Delta x$ -dendrite =  $20 \mu\text{m}$ .

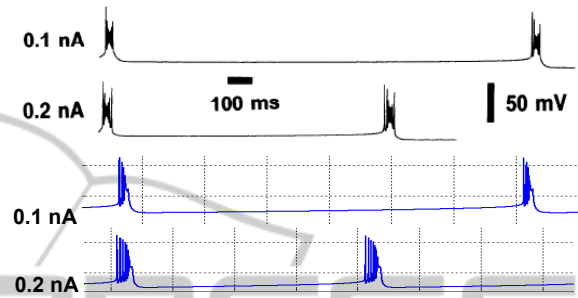


Figure 8: Burst replication of biological neuron recordings (top) with the two-compartment model proposed (bottom). Dashed square on simulation represents  $50\text{mV} \times 200\ \text{msec}$ .

## 5 CONCLUSIONS

A detail dynamics analysis for the two-compartment Traub model was developed, taking into consideration that this model is used in hardware-based applications. So the numerical method and data representation must be taken into account, in contrast with previous analysis which use software-based PC simulators and where these implementations details are not considered.

The presented hardware-based model is able to reproduce biological meaningful information, dynamic behaviour and it is suitable to reproduce neuron recording experiments.

The leakage conductance and current applied can be used to tune neuron to a non-bursting resting state. Both options were selected because they do not compromise the dynamics of the original model.

Through the analysis, two different applied currents were considered: short duration and long steady. For a short duration current, seven different types of burst patterns were detected and analysed. Also, it was detected that the transformation of such bursts follows a specific sequence of patterns.

When a long steady current vary, the modification of the membrane voltage trace was classified in five different stages; where VLF burst, single periodic spikes, low frequency periodic burst and modulated single spikes can be generated with particular set of values. Also it was found that geometric parameters

can influence in frequency and amplitude of neuron response.

Specific parameters values of current applied and morphological dimensions can be used to generate different burst patterns or to move from one stage to another when a specific firing frequency is required.

As future work, it is intended to use this information for parameter self-tuning genetic algorithm experiments and replicate living cells recordings and study the influence of biological-compatible parameters. In addition, dynamics analysis will be extended to other parameters, mainly to ion-channel maximum conductances and inhibitory/excitatory synapses, in order to use this information in a conductance-based neural network learning algorithm.

The final goal is to build biophysically compatible neurons that fit on single chips and have biological meaningful information that matches behaviour of real cells, in order to biologist have alternative ways to study physical nervous systems in a configurable, well-controlled and real-time environment.

## REFERENCES

- Booth, V. and A. Bose (2002). "Burst synchrony patterns in hippocampal pyramidal cell model networks." *Network* 13(2): 157-177.
- Bower, J. M. and D. Beeman (1998). "The book of GENESIS." Springer-Verlag New York, Inc.
- Coombes, S. and P. C. Bressloff (2005). *Bursting The Genesis of Rhythm in the Nervous System*, world Scientific Printers.
- Dayan, P. and L. F. Abbott (2001). *Theoretical neuroscience: computational and mathematical modeling of neural systems*, MIT.
- Fei, X. Y., Jiangwang and L. Q. Chen (2006). "Bifurcation control of Hodgkin-Huxley model of nerve system." *WCICA 2006: Sixth World Congress on Intelligent Control and Automation*, Vols 1-12, 9406-9410.
- Feng, J. F. and G. B. Li (2001). "Behaviour of two-compartment models." *Neurocomputing* 38: 205-211.
- Grzywacz, N. M. and P.-Y. Burgi (1998). "Toward a Biophysically Plausible Bidirectional Hebbian Rule." *Neural Computation* 10(3): 499-520.
- Guckenheimer, J. and I. S. Labouriau (1993). "Bifurcation of the Hodgkin and Huxley Equations - a New Twist." *Bulletin of Mathematical Biology* 55(5): 937-952.
- Hodgkin, A. L. and A. F. Huxley (1952). "A quantitative description of membrane current and its application to conduction and excitation in nerve." *J Physiol* 117(4): 500-544.
- Jiang, W., G. Jianming and F. Xiangyang (2005). "Two-parameter Hopf bifurcation in the Hodgkin-Huxley model." *Chaos, Solitons & Fractals* 23: 973-980.
- Kepecs, A. and X. J. Wang (2000). "Analysis of complex bursting in cortical pyramidal neuron models." *Neurocomputing* 32: 181-187.
- Khan, G. M. and J. F. Miller (2010). "Learning Games using a Single Developmental Neuron." *Proc. of the Alife XII Conference(University of York)*.
- Moctezuma, J. C., J. P. McGeehan and J. L. Nunez-Yanez (2013). Numerically efficient and biophysically accurate neuroprocessing platform. *Reconfigurable Computing and FPGAs (ReConFig)*, 2013.
- Pinsky, P. F. and J. Rinzel (1995). "Intrinsic and network rhythmogenesis in a reduced Traub model for CA3 neurons." *Journal of Computational Neuroscience* 2(3): 275-275.
- Rinzel, J. and R. N. Miller (1980). "Numerical-Calculation of Stable and Unstable Periodic-Solutions to the Hodgkin-Huxley Equations." *Mathematical Biosciences* 49(1-2): 27-59.
- Schwartzkroin, P. A. (1975). "Characteristics of CA1 neurons recorded intracellularly in the hippocampal in vitro slice preparation." *Brain Res* 85(3): 423-436.
- Smaragdou, G., S. Isaza, M. F. v. Eijk, I. Sourdis and C. Strydis (2014). "FPGA-based biophysically-meaningful modeling of olivocerebellar neurons". *ACM/SIGDA international symposium on FPGAs*. Monterey, California, USA, ACM: 89-98.
- Traub, R. D. (1982). "Simulation of intrinsic bursting in CA3 hippocampal neurons." *Neuroscience* 7(5): 1233-1242.
- Traub, R. D., J. G. Jefferys, R. Miles, M. A. Whittington and K. Toth (1994). "A branching dendritic model of a rodent CA3 pyramidal neurone." *J Physiol* 481 ( Pt 1): 79-95.
- Traub, R. D., R. K. Wong, R. Miles and H. Michelson (1991). "A model of a CA3 hippocampal pyramidal neuron incorporating voltage-clamp data on intrinsic conductances." *J Neurophysiol* 66(2): 635-650.
- Wang, J., J. M. Geng and X. Y. Fei (2005). "Two-parameters Hopf bifurcation in the Hodgkin-Huxley model." *Chaos Solitons & Fractals* 23(3): 973-980.
- Wang, L., S. Liu, J. Zhang and Y. Zeng (2012). "Burst firing transitions in two-compartment pyramidal neuron induced by the perturbation of membrane capacitance." *Neurol Sci* 33(3): 595-604.
- Zhang, Y., J. Nunez and J. McGeehan (2010). "Biophysically Accurate Floating Point Neuroprocessors." *University of Bristol*.